SED-Vol. 16, Wind Energy – 1995
ASME 1995

FATIGUE OF FIBERGLASS BEAM SUBSTRUCTURES

John F. Mandell, David W. Combs, and Daniel D. Samborsky
Department of Chemical Engineering
Montana State University
Bozeman, Montana 59717

ABSTRACT

Composite material beams representative of wind turbine blade substructure have been designed, fabricated, and tested under constant amplitude flexural fatigue loading. Beam stiffness, strength, and fatigue life are predicted based on detailed finite element analysis and the materials fatigue database developed using standard test coupons and special high frequency mini-coupons. Beam results are in good agreement with predictions when premature adhesive and delamination failures are avoided in the load transfer areas. The results show that fiberglass substructures can be designed and fabricated to withstand maximum strain levels on the order of 8000 microstrain for about 10^6 cycles with proper structural detail design and the use of fatigue resistant laminate constructions. The study also demonstrates that the materials fatigue database and accurate analysis can be used to predict the fatigue life of composite substructures typical of blades.

INTRODUCTION

The overall goal of the fatigue program at Montana State University is to provide a full treatment of the fatigue performance of composite materials for wind turbine blades. The program includes studies covering the spectrum from fundamental characterization and modelling of basic elements of the materials, through the prediction and testing of typical industry laminates, to the study of material response in the context of representative substructures typical of blades. The program will be extended in future work to include material performance in service for both small experimental blades and interaction with full scale commercial blade tests.

The results of the test program have been presented in recent papers and reports [1-3], and current details will soon be available in two subcontractor reports [4,5]. This paper presents a summary of recent efforts in the substructure area, including the development of a representative substructure beam and testing capability. The goal is to characterize the materials at a simple, generic level, predict the response of more typical laminates in fatigue, and then use these data with a detailed finite element analysis (FEA) to predict the fatigue response of the beam substructure. The prediction includes beam stiffness and strain distribution, static response, damage development, and fatigue lifetime. The results presented here are limited to constant amplitude fatigue loading, but the ongoing program will include spectrum loading as well as the performance of experimental blade structures under actual wind loading.

FATIGUE DATABASE

The fatigue behavior of the materials used in the beam substructure was characterized at two levels. First, small volume, unidirectional minicoupons loaded parallel to the fibers [2] were tested at high frequency out to 10^8 cycles. A full range of tension and compression load conditions have been covered ($R = 0.1, 0.5, -1, 2, 10$, where R is the

This work was supported by the U.S. Department of Energy through the Montana DOE EPSCoR, Sandia National Laboratories Subcontract 40-8875 and National Renewable Energy Laboratory Subcontract XF-1-11009-5. Materials were supplied by Phoenix Industries, Northern Power Systems, U.S. Windpower, and Hexcel. Supercomputing time was provided by the Illinois NSF Supercomputing Center.

ratio of minimum to maximum stress). Second, standard size coupons of a similar laminate layup to that of the beams were tested in fatigue at R=0.1 and 10 to moderate cycles. These and the high frequency data are shown later in direct comparison with beam flange performance. The complete database for high frequency and standard laminate tests can be found in References 1-5.

BEAM SUBSTRUCTURES, TESTING, AND ANALYSIS

Figures 1 and 2 show the beam substructures developed in this program. These are selected to be representative of the structural characteristics of wind turbine blades as illustrated in Figure 3. In addition to the three configurations shown in Fig. 2, a fourth configuration similar to Configuration 3, but with a thicker web and triax reinforced flanges with no ply drops was also tested. Table 1 gives the construction and thicknesses for each of the eight beams tested. The materials used in the beams are defined in Table 2, with more details available in Ref. 4.

All beams reported here were assembled from resin transfer molded flanges and webs fabricated at MSU, although industry supplied materials could also be substituted for various parts of the structure.

Beam fatigue tests were run in a four-point flexural apparatus in standard servohydraulic testing machines [2]. Details of the apparatus and instrumentation can be found in Ref. 4. All beams were instrumented with strain gages on the flanges, with selected beams also instrumented for center-point deflection and web strains. Beams were inspected periodically for damage development during fatigue, and consequent stiffness changes were also monitored.

All configurations shown in Figure 2 were analyzed in detail using a three-dimensional finite element analysis (ANSYS software). The FEA results were used in the initial beam design and in developing modified designs to avoid failure in the load transfer areas. The analyses described here used average orthotropic properties for the flanges, web, etc. obtained from classical laminate theory software and verified by experimental data. The FEA mesh typically included only one element through the thickness of each flange or web section, and so gave only approximate stresses for details like the adhesive bond-lines. (Other parts of this study involve more detailed FEA of local regions of material with elements much smaller than individual strands or adhesive layers [2].)

BEAM STIFFNESS

Figure 4 gives FEA predicted stiffness and flange strain vs load for Beam 4, Configuration 3. The one-cycle data are in good agreement with the FEA prediction. This beam was also cycled in fatigue in a series of steps of increasing load, as indicated in Table 2. The beam stiffness is shown in Figure 4 to decrease with increasing cycles (center point displacement increases). This was due to repeated delamination at the ply drops, as well as other damage, as described later. No attempt was made to simulate the stiffness decrease by modelling the damage, but this will be carried out in future work, as will non-destructive evaluation of the damage. The extent of stiffness change shown in Figure 4 is related to the particular geometry of the beams used in this study, and would likely be lower in actual blade structures. The flange strain in Figure 4 does not show as much increase with cycling as does the displacement because the damage is primarily outside the gage section.

BEAM STRUCTURAL DETAIL PROBLEMS

Beams 1-3 used Configurations 1 and 2 in Figure 2. These beams all developed failures in the adhesive bond-line on the tensile flange just over the end of the shear stiffener; additional problems with load pad failure resulted in modifications to the loading fixture to include free rotation of the supports. Finite element analysis of the area near the end of the shear stiffener indicated high adhesive shear stresses, on the order of 1400 psi for a load of 4000 lb. Redesign of the shear stiffener to the geometry in Configuration 3 led to a reduction in the adhesive shear stress to less than 600 psi at 4000 lb. force, as shown in Figure 5, and adhesive failure was not a problem in Configuration 3. Load transfer at structural details becomes a greater problem with larger structures, where more force per unit of structure area must be transferred for typical layered composite structures.

A second problem with the beam structure was the ply drops indicated in Configurations 2 and 3. These were drops of individual 0° plies spaced about 1.0 in. apart. The ply drops on the tensile flange delaminated at low cycles for fatigue with maximum strains in the 6000 microstrain range. Similar delamination on the compressive flange was less severe and required higher strain or more cycles, apparently due to a negative Mode I component to the delamination. Delaminations were periodically repaired by injection of a low viscosity epoxy adhesive, but the same areas soon delaminated again. Efforts to suppress the delamination by covering the ply drops with chopped strand mat were not successful, as delaminations still developed. The ply drop delamination continues to be a problem, even for single ply drops, at least on the laminate surfaces. Delamination at ply drops does not cause catastrophic failure, but it does reduce the structure stiffness. Further study is planned for the ply drop problem; it should be noted that ply drops will probably not delaminate at the much lower strain levels currently experienced by blades in service.

BEAM FATIGUE RESULTS

Beams 1-3 failed due to adhesive failure in the load transfer area, as noted. Beam 4, Configuration 3,

performed up to expectations in fatigue with the exception of repeated ply drop delaminations, which were repaired five times during the test, then finally ignored in the last load step. Table 2 gives the block loading history for Beam 4, with blocks of cycles at increasing loads until failure. Figure 6 gives the cycles run at each load block in terms of maximum flange strains, as compared with standard coupon fatigue data in tensile fatigue (R=.1) and compressive fatigue (R=10). The beam was cycled with a load ratio of 10, so that the tensile flange experienced R=0.1 and the compressive flange R=10.

The data in Figure 6 show that Beam 4 withstood fatigue cycling with flange strains near or exceeding the cycles to fail standard coupons at similar strains. For this beam load range, both tensile and compressive flanges are predicted to be close to failure at maximum absolute strains of 8000 to 9000 microstrain and cycles of 10^5 to 10^6. Final failure was on the tensile flange, as strips of material split away, and in the web near the end of the shear stiffener. These results show that standard coupon fatigue data and FEA can be used to predict substructure lifetime if structural details are adequate to transfer sufficient load to the flanges. The compressive flange did not fail, even though coupon data marginally indicated failure in this mode (Fig. 6). Compressive coupon data were actually obtained with the 45° layer on the outside surfaces, which has now been found to lower the coupon strength significantly for coupons in this size range, due to gripping restraints. Thus, it is expected that improved coupon data would have raised the coupon S-N curve slightly relative to that in Fig. 6. Compressive beam failures are generally expected in the lower cycle, higher load range, and this will be explored in the future. Beam 5, in the same geometry as Beam 4, was failed in a static test (Figure 7) and produced a compressive flange failure at a load of 21345 lb. and a strain of about 1700 microstrain shown on Figure 6. (The actual failure mode included significant web damage as well.) Thus, the static failure was at a compressive flange strain slightly above the coupon data range of 1300 to 1600 microstrain, but close to the expected range.

The data for Beam 4 have also been compared with the predictions from the minicoupon, high frequency tests. These tests are run on specimens 0.25 in. wide and one or two plies thick, using typical reinforcing fabrics and polyester matrix [5]. The small volume of material reduces hysteretic heating problems, allowing high frequency (100Hz) fatigue tests to be run to obtain a high cycle database. The small specimens have well aligned reinforcement and a high fiber content, V_f=.50 to .70. The high frequency database has been found to correlate with standard one to two inch wide coupon S-N curves if the stress data are normalized by the static (one-cycle) strength or strain to failure, using the appropriate tension or compression tests. Figure 8 gives the normalized high-frequency R=.1 and 10 data sets along with the Beam 4 final four loading steps, each normalized by the appropriate static tension or compression strength from coupon tests on the flange materials. The results in Figure 8 indicate that the high frequency database provides a good prediction of beam lifetime. A note of warning: the high frequency database should only be used for laminates with separate 0° and ± 45° or other off-axis plies. It will give a very non-conservative prediction in tension for most stitched triax or woven fabric reinforcements, as demonstrated in the following. The fabric used in the flanges of Beams 1-5 were Knytex D155 and DB240. Recent results also show that laminates with separate 0° and ±45° layers may have poor fatigue resistance at higher fiber volume fractions. It is advisable to obtain standard coupon data for any laminate under consideration.

Six beams have also been tested using flanges of stitched triax reinforcement, Knytex CDB200. This fabric is the most fatigue resistant triax tested to date, but is substantially more fatigue sensitive in tension than the separate 0° and ±45° plies used in Beams 1-5. Beams 6-12 followed Configuration 3, but with no ply drops and a slightly thicker web construction (Table 1). Beams 7, 8, 11 and 12 were tested in fatigue and failed due to tensile flange failure as predicted (Fig. 7). Beams 6 and 9 were tested statically, and failed due to compression flange failure (similar to Beam 5), at a strain somewhat below the coupon failure strain. The flanges on Beams 6-12 were only 0.1 in. thick, and the compressive static failure may have been partially due to flange buckling instability; this is being explored currently. Figure 9 shows good agreement between the standard coupon fatigue S-N curves for this fabric and the flange strains and cycles which produced beam failure. The fatigue failure strains for beams with triax flanges are signifcantly lower than for flanges with separate 0° and ±45° layers, as predicted (Fig, 6 vs. Fig, 9). As noted above, the high frequency data for tensile fatigue in Figure 8 would significantly overpredict the tensile flange lifetime with this triax fabric. Figure 9 indicates the anticipated transition from compression flange failure at low cycles/high loads to tensile flange failure at higher cycles/lower loads. This transition is particularly pronounced for triax materials, but is also predicted and observed for laminates with separate 0° and ±45° layers.

Further validation of the use of the fatigue database and FEA to predict substructure performance over a broader load and materials range is planned for the future, including spectrum loading.

CONCLUSIONS

Substructure beams representative of blade structure have been fabricated and tested in four-point flexural fatigue loading. The established materials database

coupled with finite element analysis have been used to predict beam stiffness, strength, and lifetime.

Difficulties were encountered with adhesive/delamination failures in structural details involving load transfer and ply drops. Redesign of the beams eventually produced structures capable of loading the beam flanges to failure under static and fatigue loading. Experimental data for beam fatigue performance are in good agreement with predictions, including failure mode. The high frequency database can be used to predict structure lifetime for laminates with with good fatigue performance, but not for laminates such as stitched triax. Beams with triax reinforced flanges fail at lower strains, as predicted from coupon data.

REFERENCES

1. J.F. Mandell, R.M. Reed, D.D. Samborsky, and Q. Pan, "Fatigue Performance of Wind Turbine Blade Materials" in SED-Vol 14, Wind Energy 93, S. Hock, ed, ASME, New York, p.p. 191-198 (1993).
2. J.F. Mandell, R.F. Creed,Jr., Q. Pan, D.W. Combs, and M. Shrinivas, "Fatigue of Fiberglass Generic Materials and Substructures" in SED-Vol 15, Wind Energy 94, W.D. Musial, S.M. Hock, and D.E. Berg, eds., ASME, New York, p.p. 207-213 (1994).
3. J.F. Mandell, R.M. Reed, and D.D. Samborsky, "Fatigue of Fiberglass Wind Turbine Blade Materials" Contractor Report SAND92-7005, Sandia National Laboratories, Albuquerque, N.M. (1992).
4. J.F. Mandell, D.W. Combs, D.D. Samborsky, and Q.Pan, "Fatigue of Composite Structures" Final Report on NREL Subcontract XF-1-11009-5 (to be published).
5. J.F. Mandell, R.F. Creed,Jr., A.J. Belinky, and G. Wei, "Fatigue of Fiberglass Generic Wind Turbine Materials" Final Report on Sandia Subcontract 18-3958 (to be published).

Part	Lay-up	Thickness (in.)
Beams 4,5		
Pads	$[(0/90)_4]_s$	0.35
Shear Stiffener	$[(\pm 45)_3]_s$	0.35
Web	$[(\pm 45)_2]_s$	0.14
Flange		
outer section	$[c.m./(0)_2/(\pm 45)/(0)_4]$	0.19
gage section	$[c.m./(0)_2/(\pm 45)/(0)_2]$	0.14
Beams 6-12		
Web	$[(\pm 45)_3]_s$	0.18
Flange	$[(\pm 45/0)_2]_s$ triax	0.10

Table 1. Lay-up schedule.

Maximum Load (lbf)	Micro-Strain	Cycles at Load	Total Cycles
5,000	3000	10,000	10,000
8,000	6000	1.16e6	1.17e6
9,000	7000	171,715	1.34e6
10,000	8000	631,360	1.97e6
11,000	9000	285,735	2.26e6

Table 2. Load, Micro-Strain and Cycles Summary, Beam 4.

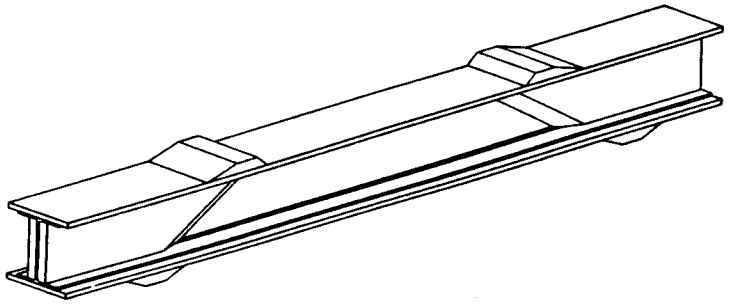

Figure 1 View of typical beam

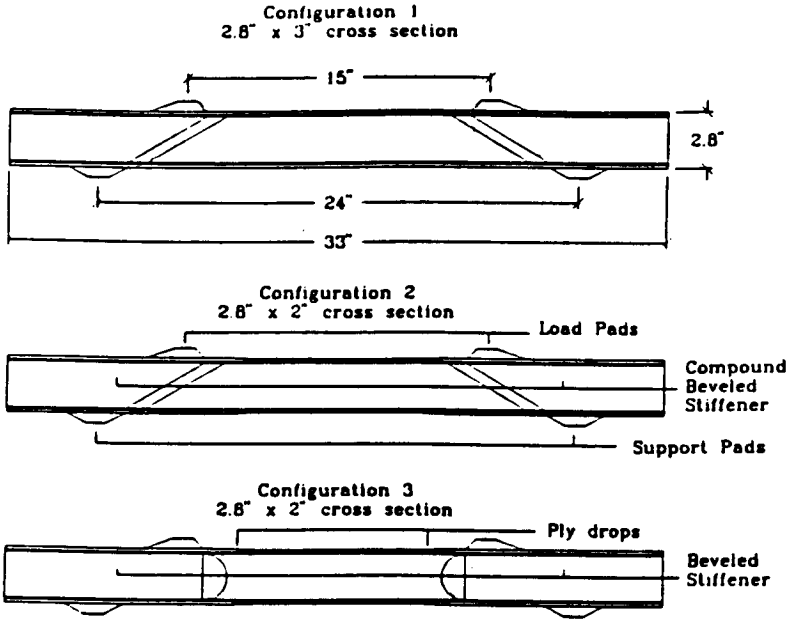

Figure 2 Beam Configurations 1,2,3

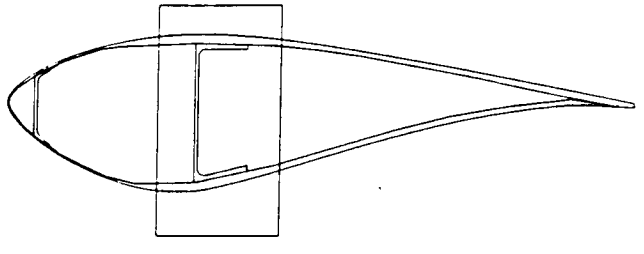

Figure 3 Blade substructure represented by beams

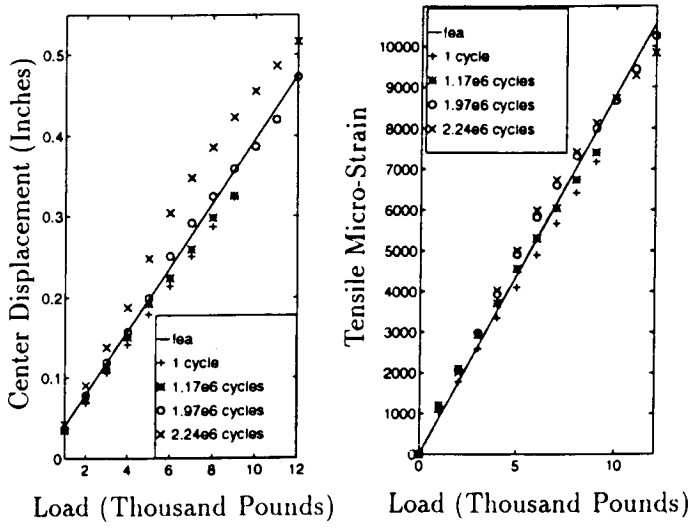

Figure 4 Beam 4 stiffness data vs. FEA prediction, load vs. displacement (left) and load vs. flange strain (right)

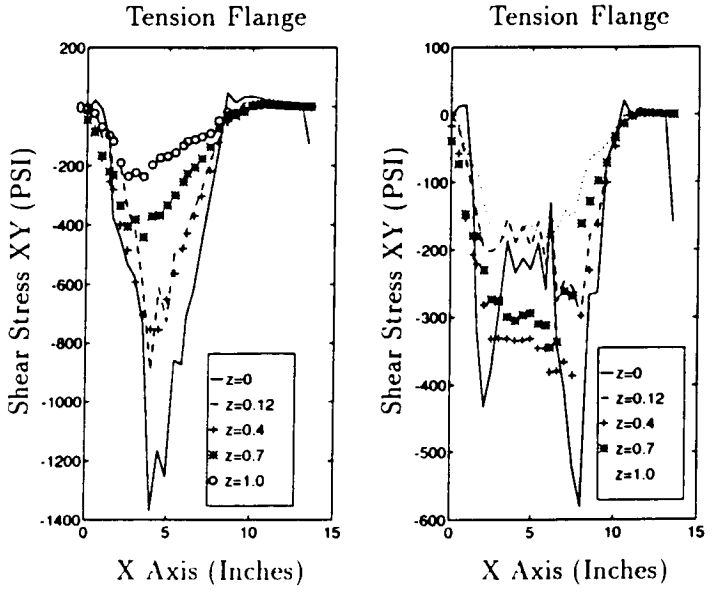

Figure 5 FEA results for shear stress between flange and web, Beam Configuration 2 (left) vs. 3 (right)

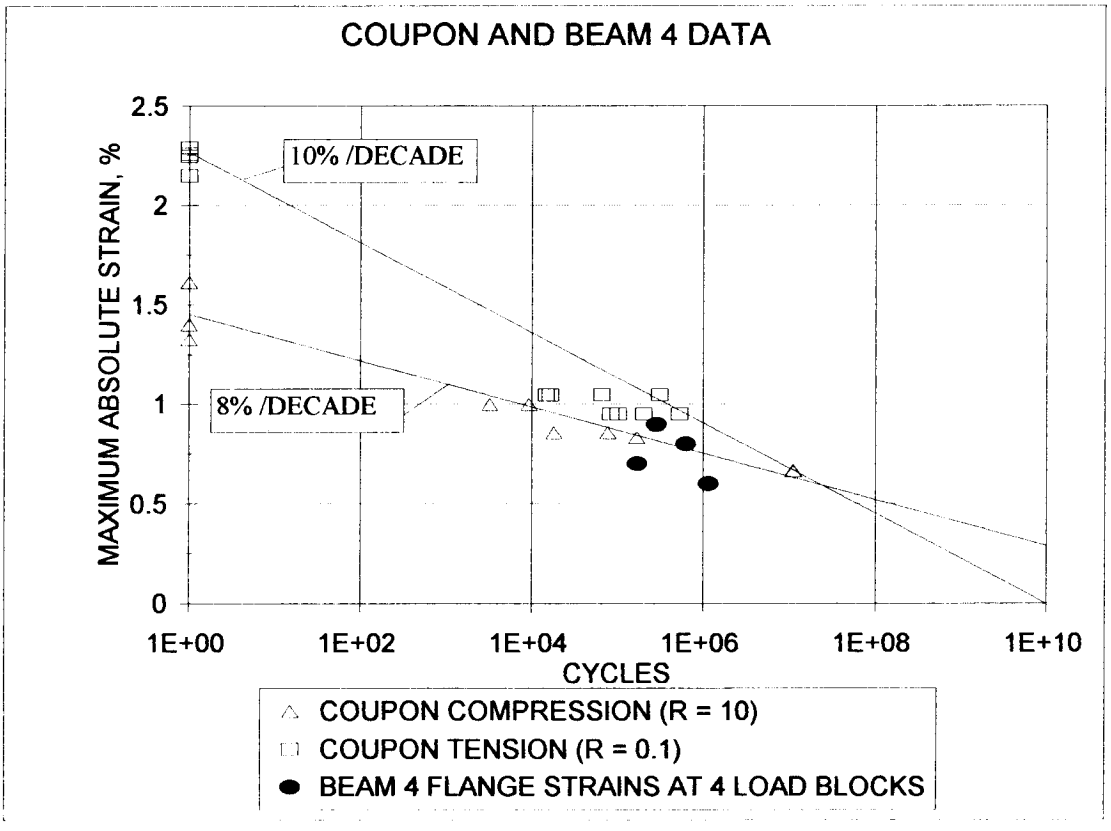

Figure 6 Beam 4 fatigue data for flange strains vs. coupon data. Each point for beam represents one load block in Table 2. Failure occurred at the highest point shown

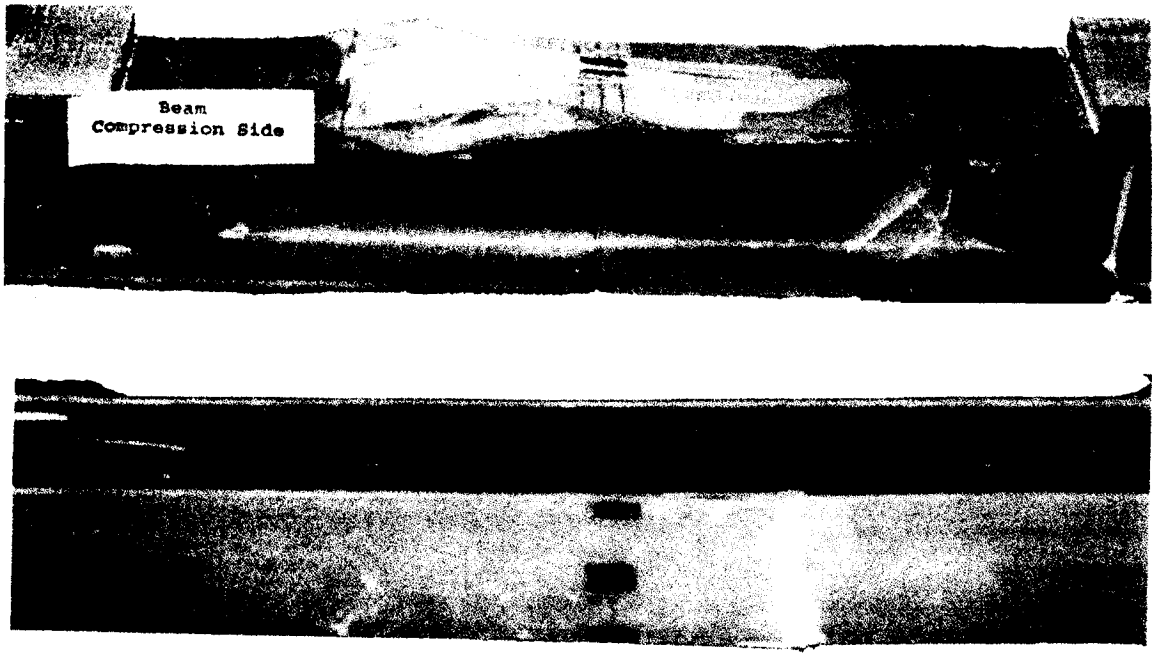

Figure 7 Static compressive/web failure of Beam 5 (top) and tensile flange failure mode of Beam 8

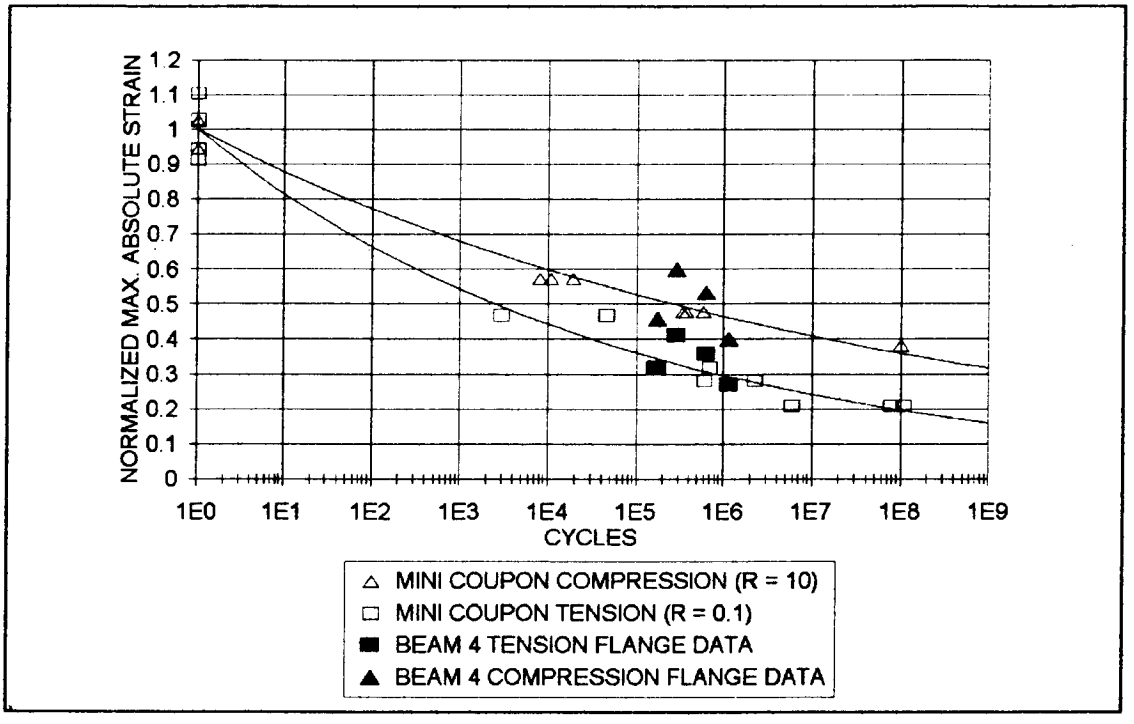

Figure 8 Normalized high frequency small specimen fatigue data vs. Beam 4 data from Table 1, normalized by flange material coupon static failure strain.

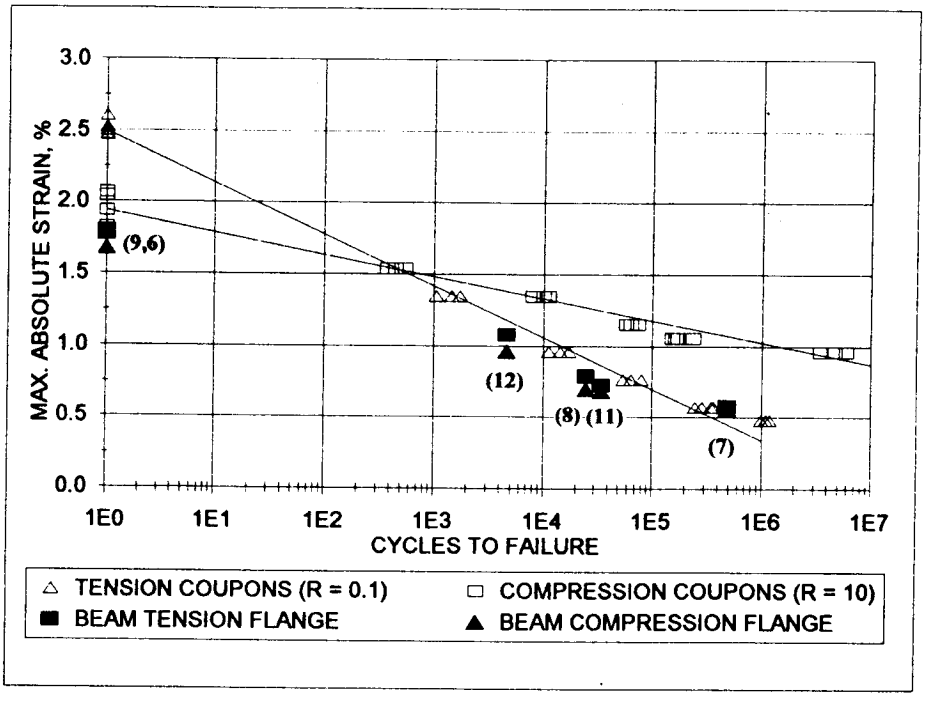

Figure 9 Fatigue data for Beams 6 through 12: flange strains compaired to standard coupon data for flange material (Triax).